



Published in final edited form as:

J Control Release. 2019 July 10; 305: 65–74. doi:10.1016/j.jconrel.2019.05.020.

Distinct Release Strategies are Required to Modulate Macrophage Phenotype in Young Versus Aged Animals

Daniel Hachim^{a,b}, Aimon Iftikhar^{a,b}, Samuel T. LoPresti^{a,b}, Alexis L. Nolfi^{a,b}, Shweta Ravichandar^{a,b}, Clint Skillen^a, and Bryan N. Brown^{a,b,c}

^aMcGowan Institute for Regenerative Medicine, University of Pittsburgh, 450 Technology Drive, Suite 300, Pittsburgh, PA 15219, United States

^bDepartment of Bioengineering, Swanson School of Engineering, University of Pittsburgh, 302 Benedum Hall, 3700 O'Hara Street, Pittsburgh, PA 15260, United States

^cDepartment of Obstetrics, Gynecology and Reproductive Sciences, University of Pittsburgh, 300 Halket Street, Pittsburgh, PA 15213, United States

Abstract

The role of innate immunity and macrophages in the host response to biomaterials has received renewed attention. A context-dependent spectrum of macrophage phenotypes are shown to affect tissue integration and performance of implanted biomaterials and medical devices. Recent studies by our group demonstrated that the host response in aged animals was characterized by delayed macrophage recruitment, differences in marker expression and a shifted pro-inflammatory (M1) response, associated with an unresolved host response in the long-term. The present work sought to study the effects of single and sequential cytokine delivery regimens in aged mice to restore delayed recruitment of macrophages and shift the inflammatory host response towards an M2-like phenotype, using MCP-1 (macrophage chemotactic protein-1) and IL-4 (interleukin-4), respectively. Implantation of cytokine-eluting implants showed a preserved response to MCP-1 in both young and aged animals, restoring delayed macrophage recruitment in aged mice. However, the response elicited by IL-4, sequential delivery of MCP-1/IL-4 and coating components was distinct in young versus aged mice. While single delivery of IL-4 did not counteract the high inflammatory response observed in aged mice, the sequential delivery of MCP-1/IL-4 was capable of restoring both recruitment and shifting the macrophage response towards an M2-like phenotype, associated with decreased implant scarring in the long-term. In young mice, sequential delivery was not as effective as IL-4 alone at promoting an M2-like response, but did result in a reduction of M1 macrophages and capsule deposition downstream. These results demonstrate that a proper understanding of patient/context-dependent biological responses are needed to design biomaterial-based therapies with improved outcomes in the setting of aging.

Corresponding author: Bryan Nicklaus Brown. McGowan Institute for Regenerative Medicine, University of Pittsburgh, 450 Technology Drive, Suite 300, Pittsburgh, PA 15219, United States. Phone: (412) 624-5273. brownb@upmc.edu.

Publisher's Disclaimer: This is a PDF file of an unedited manuscript that has been accepted for publication. As a service to our customers we are providing this early version of the manuscript. The manuscript will undergo copyediting, typesetting, and review of the resulting proof before it is published in its final citable form. Please note that during the production process errors may be discovered which could affect the content, and all legal disclaimers that apply to the journal pertain.

Keywords

Host response; biomaterials; aging; cytokine; macrophage; IL-4; MCP-1; sequential; delivery

Introduction

Macrophages are considered to be key mediators of the success or failure of implanted biomaterials due to their regulatory role in numerous phases of the host response to implants [1-3]. The classically defined host response to biomaterials begins immediately upon implantation and proceeds in phases which include protein adsorption, acute inflammation, chronic inflammation, foreign body reaction and eventual fibrotic encapsulation of the implant [4]. It is now understood that the macrophages which participate in the host response to implantable materials can adopt multiple phenotypic and functional profiles contained in a continuum between multiple extremes, including pro-inflammatory (M1) and pro-regenerative (M2) phenotypes, among others [5-10]. Characterization of the macrophage response to biomaterials has shown that materials that elicit a predominantly M1-type response are associated with poor remodeling outcomes compared to those which elicit a more M2-type or mixed M1/M2 response. Specifically, a persistent inflammatory M1 response has been associated with tissue degradation, scarring and downstream complications [11-14]. On the other hand, better remodeling outcomes have been observed when the early host response shifts from an initially M1 to a more M2-like profile. These improved outcomes can include enhanced integration, new site-appropriate and functional tissue formation, depending upon the material and location of the implant [15-20].

For these reasons, an increasing number of studies in biomaterials and regenerative medicine have begun to use macrophage modulation as an approach to improve tissue remodeling, biomaterial integration and functional recovery, with promising results. These studies have demonstrated that remodeling outcomes are improved when M2-polarizing cytokines such as IL-4 (interleukin-4) and IL-10 (interleukin-10) are delivered to the implantation site, while the opposite is observed for M1-polarizing cytokines such as IFN- γ (interferon- γ) [21-24]. Other studies have demonstrated the importance of both M1 and M2 responses, and a timely transition from M1 to M2 phenotypes, by showing enhanced vascularization and remodeling of bone scaffolds that promoted an M1 response followed by an M2 response via sequential delivery of IFN- γ and IL-4, respectively [23]. A recent study by our group demonstrated that shifting the macrophage response towards an M2 phenotype at the tissue-implant interface during the first two weeks post-implantation via delivery of IL-4 mitigated the foreign body reaction and improved implant integration of polypropylene mesh implants downstream [25].

While such approaches have shown promise for improving outcomes associated with biomaterial implantation, their success is likely predicated upon an understanding of the local tissue environment and disease context in which the materials are used. Aging represents one such context. Aging is accompanied by an unavoidable decline in physiological function known to affect multiple aspects of the immune system and is highly associated with age-related disorders such as diabetes, cancer and cardiovascular disease

[26-30]. Macrophages, central effectors of the innate immune system and primary responders to biomaterial implants, have been demonstrated to elicit impaired responses in both the response to infection and tissue regeneration following injury in aged individuals and animal models [31-34]. In particular, aging has shown to have the strongest impact upon the function of tissue-resident populations, while the activity of bone-marrow derived macrophages remains largely intact [33-35]. Therefore, understanding the impact of aging and related concomitant disorders in the host response to implanted biomaterials is instrumental for the success of biomaterial-based therapies and devices in an increasingly aged population. In a recent study, we examined the impact of aging on the host response to polypropylene mesh implanted subcutaneously in 2-month and 18-month old mice [35]. The results of this study demonstrated that, while macrophages derived from the bone marrow of aged animals were largely functionally intact and were able to effectively polarize towards both an M1 and M2 phenotype, macrophage polarization observed at the tissue level was markedly different. The host response in aged mice was characterized by delayed cell recruitment, significant differences in macrophage marker expression, a highly shifted pro-inflammatory (M1) response in tissue macrophages at early stages, and an unresolved host response in the long-term as compared to young mice. This mimics delays in cellular and immune infiltration observed in aged wound healing, which has been associated with a decline in chemokine levels in aged mice [36-38]. In addition, there has been shown to be impaired activation of macrophages to the M2 phenotype in aged mice previously [30, 39, 40].

For these reasons, we hypothesized that a revised strategy for cytokine delivery would be required in aged animals to account for the observed delays in cellular recruitment and the predominantly pro-inflammatory polarization observed in aged animals compared to young. The present study examines the ability of a sequential delivery regimen for aged mice to restore the delayed recruitment of functionally intact, circulation-derived macrophages and shift the highly inflammatory macrophage response towards an M2-like phenotype, using MCP-1 (macrophage chemoattractant protein-1) and IL-4, respectively. To do so, we have developed a multi-layered nanometric coating for concomitant and sequential delivery of MCP-1 and IL-4. In addition, we have studied the effect of multiple delivery regimens in the host response of both young and aged mice to demonstrate how the biological context of an aged microenvironment and a targeted design affect the performance of biomaterial-based approaches.

Material and methods

Materials.

A polypropylene mesh, Gynemesh® PS (Ethicon, Somerville, NJ) was used. Maleic anhydride, chitosan (low molecular weight, deacetylation degree 85%), dermatan sulfate (chondroitin sulfate B, from porcine intestinal mucosa, 90% purity), chitosanase, chondroitinase ABC, bovine serum albumin (BSA) and histologic staining materials were purchased from Sigma Aldrich (St. Louis, MO). Murine IL-4, MCP-1 and ELISA kits were purchased from Peprotech (Rocky Hill, NJ), all with 98% purity by SDS-PAGE and HPLC analyses. Rabbit anti-mouse arginase (Arg-1, cat. ab91279), inducible nitric oxide synthase

(iNOS, cat. ab3523), and anti-rabbit, anti-rat Alexa-fluor (donkey) secondary antibodies were purchased from Abcam (Cambridge, MA). Rat anti-mouse F4/80 (cat. MCA497R) was purchased from ABD Serotec (Raleigh, NC). DAPI and Milli-Q water were purchased from Thermo Fisher Scientific (Pittsburgh, PA).

Plasma treatment and Layer by Layer coating of polypropylene meshes.

Polypropylene (PP) meshes were cleaned using a 1:1 acetone:isopropanol mixture and then air dried prior to irradiation with 15 seconds of argon plasma at 600W, an argon gas flow of 35 mL/min and a steady state pressure of 250 mTorr (50 mTorr initial pressure) using an Ion 40 Gas Plasma System (PVA Tepla America, Inc) to induce a surface charge which enabled layer by layer deposition as previously described [41]. Maleic anhydride powder (1.5 gr) was placed into a glass plate inside of the machine chamber. 1 cm² pieces of PP mesh were then placed around the plate to a distance of 8.5 cm. After an initial pressure of 50 mTorr was reached, 30 seconds of maleic anhydride plasma treatment was performed at 600W, an argon gas flow of 35 mL/min and a steady state pressure of 250 mTorr. Finally, PP meshes were rinsed for 30 minutes with milli-Q water and then boiled for 20 minutes in fresh milli-Q water.

Coating was performed in a customized and automated dipping instrument (8-position SILAR coating system, PTL-SC-6A. MTI Corporation, Richmond, CA). 1 cm² pieces of PP mesh were dipped in chitosan (2 mg/mL in 0.5% acetic acid) for 10 minutes at RT, then washed three times (1-minute each) in milli-Q water. Next, meshes were dipped in a dermatan sulfate solution (2 mg/mL in water) for 10 minutes at room temperature. Meshes were washed again three times in milli-Q water. This cycle was repeated until a core coating of 10 bilayers (PP-[CH/DS]₁₀) was achieved. After coating, meshes were lyophilized and stored at 4°C until further treatment to achieve cytokine loading as described below.

MCP-1 and IL-4 loading and release assays.

Dermatan sulfate (2 mg/mL) was incubated overnight at 4°C with IL-4 (1.5 µg/mL) or MCP-1 (0.75 and 1.5 µg/mL) prior to coating. For concomitant and sequential regimens, both MCP-1 (0.75 µg/mL) and IL-4 (1.5 µg/mL) were added to dermatan sulfate (2 mg/mL) and incubated overnight at 4°C. Then, polypropylene meshes with a 10-bilayer core coating were further coated with 40 bilayers containing IL-4 or 20 bilayers containing MCP-1. For concomitant and sequential delivery, core-coated meshes were further coated with 20 bilayers containing IL-4 and then coated with 20 additional bilayers containing both MCP-1 and IL-4. After coating, cytokine-loaded meshes were lyophilized and stored at -20°C. All mesh materials were then terminally sterilized using ethylene oxide and stored at -20°C before use.

Immunolabeling was used to qualitatively demonstrate the loading and distribution of IL-4 and MCP-1 throughout the coating. Cytokine eluting meshes and controls were immersed in a 1% BSA solution to block non-specific adsorption of antibodies (1h, RT). Washing was performed in between each step by dipping the meshes four times in 0.05% Tween 20. Then meshes were immersed and incubated in a solution of rabbit anti-murine IL-4 or MCP-1 as primary antibody (1:100 in 0.1% BSA, 2 hours, RT). Meshes were then immersed in a

solution of anti-rabbit-Alexa Fluor 546 as a secondary antibody (1:100 in 0.1% BSA, 30 min, RT). Mesh fluorescence was observed under confocal microscopy (Leica DMI4000 B, Buffalo Grove, IL), in which an excitation/emission of 480/520 nm was used to observe the mesh autofluorescence (green) and 561/572 nm to observe the specific fluorescence due to the loaded IL-4 or MCP-1 (red).

Loading efficiency and release assays were performed by ELISA (Peprotech) following manufacturer instructions for both IL-4 and MCP-1. First, 1 cm² pieces of mesh containing IL-4 (40 B), MCP-1 (20 B), IL-4/MCP-1 (20B) + IL-4 (20B) or coated (no cytokine) meshes were immersed into 400 µL of a solution 0.05 units/mL chondroitinase ABC and 0.05 units/mL chitosanase in 1X PBS. Incubation was performed to multiple time points (6 h, 1 day, 2 days and then every 2 days) at 37°C, after which 400 µL of solution were aliquoted and stored at -80°C until the end of the experiment. After collection, replacement with fresh solution was performed to continue the release assay. To perform the ELISA assays, 100 µL aliquots were used from each sample at each time point. Ratio of release was calculated from the amount of cytokine released at each time point divided the total amount cytokine released at the end of the experiment (plateau in the curve).

Mouse implantation model.

An implantation model with C57BL/6J female mice (2 months and 18 months old) was used following proper housing and treatment procedures approved by the Institutional Animal Care and Use Committee (IACUC) of the University of Pittsburgh. NIH guidelines for the care and use of laboratory animals were observed. A midline incision was made and a subcutaneous pocket was created in the abdomen of each mouse in order to implant a 1 cm² piece of polypropylene mesh. 4-0 polyglycolide co-polycaprolactone (PGCL) sutures were used to close the incision, then 0.5 mg/kg of Baytril and 0.2 mg/kg of Buprenex were administered for 3 days as antibiotic and analgesic, respectively. Buprenorphine (Buprenex), an opioid analgesic, has been studied and shown not to exert any effects nor alterations in the immunological response, both acutely and chronically administered [42, 43]. After 3, 7 or 90 days, mice were euthanized and skin/mesh/muscle tissue complexes were harvested and fixed for 72 hours in neutral buffered formalin. Finally, fixed tissues were paraffin embedded and cross-sections of 7 µm were used for histological studies.

Histologic staining and evaluation.

Paraffin embedded tissue cross-sections were used for H&E and Masson's Trichrome staining. H&E and Masson's Trichrome stained tissue sections were imaged on a Nikon Eclipse E600 microscope (Tokyo, Japan) at 10X and 20X, respectively. ImageJ (version 1.48, NIH) equipped with a color deconvolution plug-in (version 1.5) was used to quantify the collagen capsule deposition surrounding mesh fibers at 90 days (3 different single fibers per sample, N = 5 each group) in images taken from histological tissue sections stained with Masson's Trichrome. These measurements included total capsule area (total capsule area in blue minus the mesh fiber in white) and density (blue area % from the total capsule area).

Immunolabeling of histological sections.

Paraffin embedded tissue sections were deparaffinized and rehydrated in a series of xylene/ alcohol/water. Incubation with proteinase K (1X) for 10 minutes at 37°C was performed to retrieve antigens. After 3 washes in water, samples were incubated at 37°C in 50 mM of CuSO₄ in 10 mM NH₄Ac buffer pH = 5, to reduce tissue background fluorescence. Slides were washed twice in TBST (25 mM Tris buffer + 0.1% tween 20). Then, a 5% donkey serum + 2% BSA + 0.1% tween 20 + 0.1% triton X-100 solution was used as blocking agent (2 hours, RT). To immunolabel M2 macrophages, arginase-1 (1:150, rabbit) and F4/80 (1:50, rat) primary antibodies were used (overnight at 4°C), followed by anti-rabbit Alexa Fluor 594 (1:400) and anti-rat Alexa Fluor 488 (1:100) secondary antibodies (40 min at RT) in blocking buffer. To immunolabel M1 macrophages, iNOS (1:100) and F4/80 (1:50) primary antibodies were used (overnight at 4°C), followed by anti-rabbit Alexa Fluor 594 (1:100) and anti-rat Alexa Fluor 488 (1:100) secondary antibodies (40 min at RT) in blocking buffer. Vectashield with DAPI mounting media (Vector laboratories, Burlingame, CA) was used to counterstain nuclei and mount. Images of centered single fibers (3 different single fibers per sample, N = 5 each group) were taken on a Nikon Eclipse E600 microscope equipped with epi-fluorescence at 40X and cell counts were analyzed using ImageJ (version 1.51a, NIH).

Statistical analysis.

A power analysis was performed based upon previous studies using the same model to determine that n=5 animals per group were required to detect an effect of 25%, with a statistical power of at least 80% and significance level of p=0.05 [25, 35]. Comparisons of means were performed by either one-way or two-way analysis of variance (ANOVA), using at least p < 0.05 as statistical significance criteria followed by Tukey's test to compare groups and Sidak's test to compare time points. Shapiro-Wilk was used to test normality. All statistical tests were performed on GraphPad Prism V7 (La Jolla California, USA).

Results and discussion

The present study utilizes a previously developed multi-layered coating technology to provide controlled and sequential delivery of both IL-4 and MCP-1. Our previous studies have shown that IL-4 can be loaded into the coating in a uniform manner throughout the entire surface of the mesh implant [25]. We have additionally shown that the released IL-4 is bioactive and that the amount and length of release can be increased by simply adding more bilayers. Chitosan, the only polycation of natural origin, has been used as a component of the coating due its excellent film deposition properties, biocompatibility and selective degradation by macrophages, which express chitinase-like enzymes [44-46]. Dermatan sulfate has been used because it binds and enhances the activity of anti-inflammatory cytokines and growth factors that include IL-4 and FGF-2, respectively [47, 48]. In the present study, an increase of macrophage recruitment in the first week post-implantation was desired based upon previous studies in mice showing that the macrophage response predominates during the first week, and then starts to decline to allow the regenerative phase to initiate [4, 23, 25, 35, 49, 50], and therefore this is a key time frame for macrophage phenotype modulation.

MCP-1 bioactivity, dosing and release assays.

Preliminary studies were performed to demonstrate the ability to load and control the release of MCP-1, as well as to elicit the desired increase in cellular recruitment to the site of implantation. Similar to IL-4 loading which has been previously described, MCP-1 can be incorporated into the mesh coating by incubation with dermatan sulfate prior to layer-by-layer coating [25]. Additionally, we have demonstrated that the length of release and amount of MCP-1 is also dependent on the number of coating bilayers in a manner previously observed for IL-4 [25]. Confocal microscopy confirmed that MCP-1 is uniformly distributed through the entire surface of the mesh (Figure 1a). Release assays confirmed that the full release of MCP-1 using 20-bilayers (coating solution containing 1.5 µg/mL of MCP-1) of coating was achieved within approximately 8 days (Figure 1c). Despite using the same concentration of loading solution, 20-bilayers of MCP-1 eluted higher amounts of cytokine than 20-bilayers of IL-4 [25]. Even though these two cytokines have similar molecular weights (13.5 kDa for IL-4 and 13.8 kDa for MCP-1), the isoelectric point of MCP-1 (9.3) is slightly higher than IL-4 (8.18), and therefore the higher positive charge and potentially other structural properties may be increasing the affinity for the negatively charged dermatan sulfate.

A pilot study investigated the implantation of MCP-1 (20 bilayers, 20B) eluting meshes subcutaneously into young-adult mice, and compared to control coated (no cytokine) and pristine (non-modified) polypropylene mesh (Gynemesh®), the latter used clinically for pelvic organ prolapse repair and associated with chronic foreign body reaction and potential complications in humans [11, 12, 51]. Histological assessment three days post-implantation showed a highly exacerbated and localized cell recruitment in MCP-1 mesh implanted over pristine and control coating mesh (Figure 1b). There were also signs of inflammation and mesh erosion in Hematoxylin and Eosin (H&E) stained tissue sections, confirming that MCP-1 is bioactive after loading and mesh sterilization (Figure 1d). The dose of MCP-1 was then adjusted by decreasing the amount of MCP-1 in the coating solution from 1.5 to 0.75 µg/mL, expecting that the number of cells recruited to the tissue-implant interface would be approximately half. Release assays confirmed that the resulting loading of MCP-1 was reduced by nearly half while preserving the same length of release (Figure 1c). Although more concentrations and mechanistic studies are required to clearly demonstrate this relationship, the present results suggest that the released amount of MCP-1 is proportional to the amount of MCP-1 in the coating solution, but that the duration of release is associated with the number of bilayers used. Implantation of meshes containing 0.75 µg/mL of MCP-1 were also capable of increasing cell recruitment compared to coated (polymers only, no cytokines) and pristine meshes, but did not elicit the erosion and poor histological response associated with mesh containing a higher amount of MCP-1 (Figure 1b, d). Also, the number of recruited cells in meshes containing 0.75 µg/mL of MCP-1 were approximately a half compared to 1.5 µg/mL of MCP-1. Therefore, the following studies utilized MCP-1 meshes with 20 bilayers where the coating solutions contained 0.75 µg/mL of MCP-1.

Concomitant and sequential release of MCP-1 and IL-4.

A concomitant and sequential delivery regimen of MCP-1 and IL-4 was desired to restore the delayed macrophage recruitment and shift the highly inflammatory response towards an

M2 phenotype, respectively. Previous studies have shown that macrophages recruited at the tissue implant interface adopt a predominantly M1 phenotype [11, 12, 25, 35, 52-55]. Therefore, a sequential regimen in which MCP-1 is released alone and followed by IL-4 likely would not be as successful at reducing the inflammatory response as a regimen that delivers concomitantly both cytokines followed by single release of IL-4 thereafter.

The multilayered nature of the coating was used to provide first concomitant release of both MCP-1 and IL-4 in the 20 external layers, then followed by single release of IL-4 in the 20 internal layers of the coating (excluding a 10B core coating without cytokine). ELISA assays demonstrated that the release profile of IL-4 was similar when released from both single IL-4 and sequential IL-4/MCP-1 eluting meshes (Figure 2a). Similarly, MCP-1 release profile in both single MCP-1 and sequential IL-4/MCP-1 eluting meshes were not significantly different (Figure 2b). Sequential release was then observed by an initial concomitant release of MCP-1 and IL-4 which was followed by release of IL-4 only (Figure 2c). Eighty percent of the total dose of MCP-1 and IL-4 was released in 8 and 12 days, respectively (Figure 2d) *in vitro*. This delivery regimen will be referred to as sequential herein after.

Mesh implantation studies of single and sequential delivery regimens in young and aged mice.

The efficacy of single and sequential delivery regimens of IL-4 and MCP-1 were evaluated by subcutaneous implantation of eluting meshes containing each or both cytokines in young adult (2 month-old) and aged (18 month-old) mice. Histological assessments at 3 days post-implantation showed increased cell recruitment in all eluting meshes containing MCP-1 in both young and aged mice (Figure 3). An exception was coated (no cytokine) mesh in aged mice which resulted in the highest infiltration of cells, localized around the mesh fibers (Figure 3b). This suggests that the host response to chitosan and/or dermatan sulfate is significantly different in aged individuals, which can be modified with the addition of MCP-1 and/or IL-4.

At 7 days, cell recruitment was similar in all aged mouse groups, but still increased for young mice, suggesting that the effects of MCP-1 were more robust in the younger mice. Of note, the exacerbated cell infiltration observed in the coated (no cytokine) aged mice group diminished to similar levels observed in other groups. A study performed by Lohmann et al. [58], has shown that glycosaminoglycan-based hydrogels sequester inflammatory chemokines such as MCP-1, IL-8 and MIP-1 β , from chronic wound fluids. It may be possible that the coating also captures the inflammatory chemokines from the aged microenvironment, but instead of sequestering and diluting the cytokines in the bulk of a hydrogel, the coating concentrates all the inflammatory cytokines in the surface of the mesh biomaterial, enhancing cell infiltration. This would also be consistent with results at 7 days, where the coating has been mostly degraded and therefore both cytokine sequestering and cell recruitment have diminished. This would not be the case for young mice, where the microenvironment is not as inflammatory as in aged mice [35, 59-61]. Another potential explanation for the exacerbated response against these materials may be due to alterations in the tissue-resident populations in aged mice, as previously described [33-35].

Effects of single and sequential delivery regimens on macrophage polarization at the early-stages of the host response.

Co-immunolabeling of histological tissue sections was performed to assess the effects of each single and sequential delivery regimen on macrophage (F4/80⁺) recruitment and polarization towards M2 (Arg-1⁺ F4/80⁺, Figure S1) and M1 (iNOS⁺ F4/80⁺, Figure S2) phenotypes. Quantification revealed that all eluting coated meshes containing MCP-1 were capable of increasing F4/80⁺ macrophage recruitment at 3 days in both young adult and aged mice. Increased macrophage presence in MCP-1 mesh over pristine mesh persisted in aged mice at 7 days, while young animals showed increased macrophage infiltration from pristine mesh over all coated groups (Figure 4 a,b). Even though coated (no cytokine) mesh elicited an exacerbated recruitment of cells, this was not correlated to F4/80⁺ macrophage recruitment, suggesting that cells other than F4/80⁺ macrophages (including non-macrophage cells) participate in this response in a manner which is influenced by the aged microenvironment. An study performed in MCP-1^{-/-} KO young mice has shown that wound healing is delayed, no changes in the number of macrophages was observed [62]. Other inflammatory models where either MCP-1 or its receptor were blocked presented a lack of monocytes and macrophages at the peritoneum, indicating a context-dependent role for MCP-1 [63-65]. When considered with our findings, these results suggest that early inflammatory infiltration in aged mice may be delayed due to alterations in tissue-resident macrophages, which are later compensated by circulatory populations.

While increased macrophage recruitment was observed in both young and aged animals when implanted with MCP-1 eluting meshes, the host response to IL-4, sequential delivery of IL-4/MCP-1 and coating components was distinct in young versus aged implanted mice. M2 macrophages were quantified via colabeling sections with F4/80⁺ and Arg-1 (arginase 1; a marker of the M2 phenotype [66]). Results showed that aged mice implanted with IL-4 single eluting coatings did not have a significantly higher percent of M2 (Arg-1⁺ F4/80⁺) macrophages, compared to the pristine mesh group. However, the percentage of M2 macrophages in the sequential MCP-1/IL-4 group was significantly increased at both 3 and 7 days, compared to all groups with no IL-4 (Figure 4 c,d). Therefore, while single delivery of IL-4 was not able to counteract the high inflammatory response present in aged mice, the sequential delivery regimen of IL-4 and MCP-1 was capable of restoring recruitment and shifting the macrophage response towards an M2-like phenotype. These findings may be related to those in previous studies which demonstrated that macrophages within the implantation site were dysfunctional, while those in the bone marrow were intact [33-35]. That is, it may be necessary to recruit macrophage populations from the circulation to cause an effective polarization towards an M2 phenotype in aged animals. Of note, the half-life of circulating monocytes in humans is approximately three times longer than in mice, therefore; recruitment, tissue extravasation and turnover of human macrophages would be difficult to discern from each other [67]. In contrast, sequential delivery regimens in young mice were not as effective as IL-4 alone in promoting an M2-like response. Young mice implanted with MCP-1/IL-4 eluting mesh showed an initial increase in the percentage of M2 macrophages at 3 days, but dramatically decreased to similarly low percentages found in all groups other than IL-4 at 7 days. Therefore, IL-4 eluting mesh was the most effective regimen shifting the response towards an M2 phenotype in young mice.

To quantify M1 macrophages, co-labeling for F4/80⁺ and iNOS (inducible nitric oxide synthase; an M1 phenotype marker [66]) was performed. Results revealed differences between young and aged animals. In young mice, the percentage of M1 macrophages was similar for all groups at 3 days (Figure 4 e,f). At 7 days, the pristine mesh group presented the highest percentage of M1 macrophages, while MCP-1 mesh showed no difference from other coated groups. In aged animals, mice implanted with both pristine or MCP-1 eluting meshes presented the highest percentages of M1 (iNOS⁺ F4/80⁺) macrophages compared to all other groups. Percentage of M1 macrophages in these two groups was similar in both 3 and 7 days. This suggests that MCP-1 only affects macrophage recruitment, but does not have an effect on macrophage polarization, which is consistent with previous reports showing high expression of MCP-1 in both M1 macrophages (e.g. tissue injury and infection) [68, 69] and M2 macrophages (e.g. tumors, hepatic fibrosis) [70, 71]. Polarization towards M1 macrophages is mainly due to an inflammatory response against the polypropylene biomaterial. The increased percentage of M1 macrophages found in aged mice implanted with MCP-1 is likely a consequence of the high percentage of F4/80⁺ macrophages recruited to the surface of the biomaterial, that become M1 macrophages due to the increased inflammatory environment in aged mice [60, 72, 73].

Effects of single and sequential delivery regimens in the host response in the long-term.

The effects of macrophage recruitment and polarization via single and sequential delivery regimens in the long term were evaluated by assessment of capsule deposition at 90 days post-implantation. Histological tissue sections were stained with Masson's trichrome to reveal the presence, morphology and distribution of the fibrotic capsule surrounding the surgical mesh implant. Both young and aged mice implanted with MCP-1 mesh showed higher capsule density than all other coated groups, but similar capsule area to mice implanted with pristine mesh (Figure 5).

In young mice, only mice implanted with IL-4 eluting mesh exhibited both decreased density and area of the capsule, while the sequential regimen of MCP-1 and IL-4 was capable of decreasing capsule area alone. In aged mice, implantation of IL-4 eluting mesh was not associated with a reduction in collagen density, but presented diminished capsule area, compared to all other groups. On the other hand, the MCP-1/IL-4 group showed less dense capsules compared to all other mesh groups, but no significant differences in capsule area. In a previous study, we showed that the host response to polypropylene mesh in aged animals is not resolved by 90 days, with higher number of cells surrounding the implant [35]. To evaluate the resolution of the host response in the presence of single and sequential delivery regimens, we quantified the number of cells at 90 days. Results show that mice implanted with MCP-1 eluting mesh have similar cell numbers to the pristine mesh groups in both young and aged mice (Figure 5d, g). In aged mice, only IL-4 presented a significant reduction in the number of cells, compared to the pristine mesh group. A reduction in the number of cells was also observed in young mice implanted with both IL-4 and MCP-1/IL-4 eluting meshes, compared to pristine mesh groups.

Taking together both outcomes at early and long-term stages of the host response in aged animals, the sequential delivery of both MCP-1 and IL-4 was the only regimen capable of

shifting the response of macrophages towards an M2-like phenotype, reducing both capsule density and area in the long term, while single delivery of IL-4 did not achieve these outcomes. This further corroborates previous studies claiming that macrophages are indeed necessary for healthy tissue remodeling and implant integration [2, 23, 25]. In particular, the imbalances in macrophage response present in aged mice would make IL-4 ineffective due to either a suboptimal number of M2-like macrophages or altered response of tissue-resident macrophages to IL-4. This would suggest that the recruitment of functionally intact circulating cells may be required to produce a shift towards the M2 phenotype. On the other hand, the single delivery of IL-4 in young animals was more effective shifting macrophages towards an M2 phenotype and reducing capsule formation, compared to the sequential delivery. These outcomes may be related to an unnecessary increase in recruited macrophages promoted by MCP-1, which would make the current dose of IL-4 suboptimal to shift the macrophage response towards an M2-like phenotype.

Limitations and future directions.

Release assays were used to study the release of cytokines *in vitro* and as an estimate for release *in vivo*; however, it is currently unknown whether coating degradation and release of MCP-1 and IL-4 *in vivo* occurs in a similar manner. The implantation studies and results regarding the effects of cytokines at early stages of the host response seem to suggest that the length of *in vivo* cytokine release is shorter - with IL-4 lasting less than 14 days and MCP-1 less than 7 days, in which the effects of these cytokines are not present. Further studies will be performed using fluorescently tagged cytokines on live imaging systems to determine the release of cytokines *in vivo*. Similarly, we have investigated the effects of only 40 bilayers of IL-4 (2 ng/cm² of mesh) and 20 bilayers of MCP-1 (1 - 2 ng/cm² of mesh) on the host response against mesh, so further regimens will be evaluated based on *in vivo* release studies.

The present study used only a limited set of surface markers and makes inferences about the origin of cells based upon these markers. Further study is necessary to determine the specific origin of the cells which participate in the host response in young and aged animals as well as to clearly determine their *in vivo* phenotype and functional profile.

Another limitation inherent in the present implantation model involves differences in macrophage pathophysiology between mice and humans [74]. Leukocyte populations in C57BL/6 mice, the same strain used in this study, contain 10-25% neutrophils, 75-90% lymphocytes and approximately 2% monocytes; while humans have 50-70% neutrophils and 20-40% lymphocytes [66, 75, 76]. In addition, arginase-1 and iNOS are effective markers of M1 and M2 macrophage population in mice, but do not correlate well with macrophage phenotype in humans [77, 78]. Although the functional importance of these differences is not clear in the context of the host response to biomaterials, the results of the present study in terms of macrophage biology should be taken with caution when extrapolating to human. To address these limitations, the use of a humanized mouse model has been proposed to test the immune response to naturally-derived biomaterials, representing a promising tool to study the human host response to biomaterials *in vivo*, and a substantial step towards translation [79].

Even though degradation of the components of the coating and uptake of IL-4 is mainly performed by macrophages, other non-macrophage cells participating in the host response could potentially respond to both MCP-1 and IL-4. MCP-1 has mostly effects over migration and infiltration of macrophages and monocytes, and the effects on other immune cells participating in the host response against biomaterials has been shown to be of minor relevance [52-55, 68]. Similar to macrophages, IL-4 also shifts the response of Th cells towards a Th2 response, which can in turn lead to polarization of macrophages to an M2 phenotype, and has been associated to pro-regenerative outcomes in other materials [80]. However, these cells do not predominate at early stages the host response, and their role in the host response was not within the scope of the present study. Overall, it is clear that there are differences in the host response between young and aged animals, and that a better understanding of these differences will help to design materials and strategies which more effectively modulate the host immune response in aged individuals.

Conclusions

The present study demonstrates that layer by layer coatings can be used to provide both concomitant and sequential delivery of MCP-1 and IL-4. The concentration of cytokine in the coating solution is proportional to the amount released *in vitro*, while the number of layers influences both the amount and length of release. *In vivo* implantation of eluting meshes revealed that MCP-1 promoted cell and macrophage recruitment in both young and aged animals, restoring the delayed recruitment in the host response of aged mice. However, the host response in presence of IL-4, sequential delivery of IL-4/MCP-1 and coating components alone was distinct in young versus aged implanted mice, suggesting that the host response to chitosan and/or dermatan sulfate is significantly different in aged individuals, which can be modified with the addition of MCP-1 and/or IL-4.

While single delivery of IL-4 was not enough to counteract the high inflammatory response present in aged mice, the sequential delivery regimen of IL-4 and MCP-1 was capable of restoring recruitment and shifting the macrophage response towards an M2-like phenotype, which is associated with decreased capsule deposition in the long term. In contrast, sequential delivery regimens in young mice were not as effective as IL-4 alone which promoted an M2-like response, but were still capable of reducing inflammatory macrophage presence and capsule deposition. In addition, the exacerbated cell recruitment in aged mice implanted with coated (no cytokine) mesh was not correlated to an increase in recruitment of F4/80⁺ macrophages nor effects on polarization, suggesting that other cells influenced by the aged microenvironment may play an important role promoting this response. These results raise important questions about the design and performance of biomaterial-based therapies and devices often intended to treat elderly patients and demonstrates that a proper understanding of patient- and context-dependent biological responses have the potential to improve outcomes in aged individuals.

Supplementary Material

Refer to Web version on PubMed Central for supplementary material.

Acknowledgments

This work was supported by the National Institutes of Health (NIH) grants K12HD043441 (BNB) and R01AG055564 (BNB).

References

- [1]. Brown BN, Ratner BD, Goodman SB, Amar S, Badylak SF, Macrophage polarization: an opportunity for improved outcomes in biomaterials and regenerative medicine, *Biomaterials*, 33 (2012) 3792–3802. [PubMed: 22386919]
- [2]. Brown BN, Sicari BM, Badylak SF, Rethinking regenerative medicine: a macrophage-centered approach, *Frontiers in immunology*, 5 (2014) 510. [PubMed: 25408693]
- [3]. Miron RJ, Bosshardt DD, OsteoMacs: Key players around bone biomaterials, *Biomaterials*, 82 (2016) 1–19. [PubMed: 26735169]
- [4]. Anderson JM, Rodriguez A, Chang DT, Foreign body reaction to biomaterials, *Seminars in immunology*, 20 (2008) 86–100. [PubMed: 18162407]
- [5]. Gordon S, Taylor PR, Monocyte and macrophage heterogeneity, *Nature reviews. Immunology*, 5 (2005) 953–964.
- [6]. Mantovani A, Sica A, Sozzani S, Allavena P, Vecchi A, Locati M, The chemokine system in diverse forms of macrophage activation and polarization, *Trends Immunol*, 25 (2004) 677–686. [PubMed: 15530839]
- [7]. Mills CD, M1 and M2 Macrophages: Oracles of Health and Disease, *Critical reviews in immunology*, 32 (2012) 463–488. [PubMed: 23428224]
- [8]. Wynn TA, Chawla A, Pollard JW, Macrophage biology in development, homeostasis and disease, *Nature*, 496 (2013) 445–455. [PubMed: 23619691]
- [9]. Mosser DM, Edwards JP, Exploring the full spectrum of macrophage activation, *Nature reviews. Immunology*, 8 (2008) 958–969.
- [10]. Xue J, Schmidt SV, Sander J, Draffehn A, Krebs W, Quester I, De Nardo D, Gohel TD, Emde M, Schmidleithner L, Ganesan H, Nino-Castro A, Mallmann MR, Labzin L, Theis H, Kraut M, Beyer M, Latz E, Freeman TC, Ulas T, Schultze JL, Transcriptome-based network analysis reveals a spectrum model of human macrophage activation, *Immunity*, 40 (2014) 274–288. [PubMed: 24530056]
- [11]. Nolfi AL, Brown BN, Liang R, Palcsey SL, Bonidie MJ, Abramowitch SD, Moalli PA, Host response to synthetic mesh in women with mesh complications, *Am J Obstet Gynecol*, (2016).
- [12]. Brown BN, Mani D, Nolfi AL, Liang R, Abramowitch S, Moalli PA, Characterization of the host inflammatory response following implantation of prolapse mesh in rhesus macaque, *Am J Obstet Gynecol*, (2015).
- [13]. Liang R, Knight K, Barone W, Powers RW, Nolfi A, Palcsey S, Abramowitch S, Moalli PA, Extracellular matrix regenerative graft attenuates the negative impact of polypropylene prolapse mesh on vagina in rhesus macaque, *Am J Obstet Gynecol*, 216 (2017) 153 e151–153 e159. [PubMed: 27615441]
- [14]. Udpa N, Iyer SR, Rajoria R, Breyer KE, Valentine H, Singh B, McDonough SP, Brown BN, Bonassar LJ, Gao Y, Effects of chitosan coatings on polypropylene mesh for implantation in a rat abdominal wall model, *Tissue Eng Part A*, 19 (2013) 2713–2723. [PubMed: 23859182]
- [15]. Brown BN, Londono R, Tottey S, Zhang L, Kukla KA, Wolf MT, Daly KA, Reing JE, Badylak SF, Macrophage phenotype as a predictor of constructive remodeling following the implantation of biologically derived surgical mesh materials, *Acta Biomater*, 8 (2012) 978–987. [PubMed: 22166681]
- [16]. Brown BN, Valentin JE, Stewart-Akers AM, McCabe GP, Badylak SF, Macrophage phenotype and remodeling outcomes in response to biologic scaffolds with and without a cellular component, *Biomaterials*, 30 (2009) 1482–1491. [PubMed: 19121538]
- [17]. Fearing BV, Van Dyke ME, In vitro response of macrophage polarization to a keratin biomaterial, *Acta Biomater*, 10 (2014) 3136–3144. [PubMed: 24726958]

- [18]. Guo R, Merkel AR, Sterling JA, Davidson JM, Guelcher SA, Substrate modulus of 3D-printed scaffolds regulates the regenerative response in subcutaneous implants through the macrophage phenotype and Wnt signaling, *Biomaterials*, 73 (2015) 85–95. [PubMed: 26406449]
- [19]. Madden LR, Mortisen DJ, Sussman EM, Dupras SK, Fugate JA, Cuy JL, Hauch KD, Laflamme MA, Murry CE, Ratner BD, Proangiogenic scaffolds as functional templates for cardiac tissue engineering, *Proc Natl Acad Sci U S A*, 107 (2010) 15211–15216. [PubMed: 20696917]
- [20]. Sussman EM, Halpin MC, Muster J, Moon RT, Ratner BD, Porous implants modulate healing and induce shifts in local macrophage polarization in the foreign body reaction, *Ann Biomed Eng*, 42 (2014) 1508–1516. [PubMed: 24248559]
- [21]. Mokarram N, Merchant A, Mukhatyar V, Patel G, Bellamkonda RV, Effect of modulating macrophage phenotype on peripheral nerve repair, *Biomaterials*, 33 (2012) 8793–8801. [PubMed: 22979988]
- [22]. Reeves AR, Spiller KL, Freytes DO, Vunjak-Novakovic G, Kaplan DL, Controlled release of cytokines using silk-biomaterials for macrophage polarization, *Biomaterials*, 73 (2015) 272–283. [PubMed: 26421484]
- [23]. Spiller KL, Nassiri S, Witherel CE, Anfang RR, Ng J, Nakazawa KR, Yu T, Vunjak-Novakovic G, Sequential delivery of immunomodulatory cytokines to facilitate the M1-to-M2 transition of macrophages and enhance vascularization of bone scaffolds, *Biomaterials*, 37 (2015) 194–207. [PubMed: 25453950]
- [24]. Pajarinen J, Tamaki Y, Antonios JK, Lin TH, Sato T, Yao Z, Takagi M, Kontinen YT, Goodman SB, Modulation of mouse macrophage polarization in vitro using IL-4 delivery by osmotic pumps, *J Biomed Mater Res A*, 103 (2015) 1339–1345. [PubMed: 25044942]
- [25]. Hachim D, LoPresti ST, Yates CC, Brown BN, Shifts in macrophage phenotype at the biomaterial interface via IL-4 eluting coatings are associated with improved implant integration, *Biomaterials*, 112 (2016) 95–107. [PubMed: 27760399]
- [26]. Franceschi C, Bonafe M, Valensin S, Olivieri F, De Luca M, Ottaviani E, De Benedictis G, Inflamm-aging. An evolutionary perspective on immunosenescence, *Ann N Y Acad Sci*, 908 (2000) 244–254. [PubMed: 10911963]
- [27]. Garrido A, Cruces J, Ceprian N, Vara E, de la Fuente M, Oxidative-Inflammatory Stress in Immune Cells from Adult Mice with Premature Aging, *Int J Mol Sci*, 20 (2019).
- [28]. Stahl EC, Brown BN, Cell therapy strategies to combat immunosenescence, *Organogenesis*, 11 (2015) 159–172. [PubMed: 26588595]
- [29]. Sebastián C, Lloberas J, Celada A, Molecular and cellular aspects of macrophage aging, in: *Handbook on immunosenescence*, Springer, 2009, pp. 919–945.
- [30]. Ma Y, Mouton AJ, Lindsey ML, Cardiac macrophage biology in the steady-state heart, the aging heart, and following myocardial infarction, *Transl Res*, 191 (2018) 15–28. [PubMed: 29106912]
- [31]. Plowden J, Renshaw-Hoelscher M, Engleman C, Katz J, Sambhara S, Innate immunity in aging: impact on macrophage function, *Aging Cell*, 3 (2004) 161–167. [PubMed: 15268749]
- [32]. Linehan E, Fitzgerald DC, Ageing and the immune system: focus on macrophages, *Eur J Microbiol Immunol (Bp)*, 5 (2015) 14–24. [PubMed: 25883791]
- [33]. Stout RD, Suttles J, Immunosenescence and macrophage functional plasticity: dysregulation of macrophage function by age-associated microenvironmental changes, *Immunol Rev*, 205 (2005) 60–71. [PubMed: 15882345]
- [34]. Linehan E, Dombrowski Y, Snoddy R, Fallon PG, Kissenpfennig A, Fitzgerald DC, Aging impairs peritoneal but not bone marrow-derived macrophage phagocytosis, *Aging Cell*, 13 (2014) 699–708. [PubMed: 24813244]
- [35]. Hachim D, Wang N, Lopresti ST, Stahl EC, Umeda YU, Rege RD, Carey ST, Mani D, Brown BN, Effects of aging upon the host response to implants, *J Biomed Mater Res A*, 105 (2017) 1281–1292. [PubMed: 28130823]
- [36]. Swift ME, Burns AL, Gray KL, DiPietro LA, Age-related alterations in the inflammatory response to dermal injury, *The Journal of investigative dermatology*, 117 (2001) 1027–1035. [PubMed: 11710909]

- [37]. Arnardottir HH, Dalli J, Colas RA, Shinohara M, Serhan CN, Aging delays resolution of acute inflammation in mice: reprogramming the host response with novel nano-proresolving medicines, *J Immunol*, 193 (2014) 4235–4244. [PubMed: 25217168]
- [38]. Lefebvre JS, Maue AC, Eaton SM, Lanthier PA, Tighe M, Haynes L, The aged microenvironment contributes to the age-related functional defects of CD4 T cells in mice, *Aging Cell*, 11 (2012) 732–740. [PubMed: 22607653]
- [39]. Mahbub S, Deburghraeve CR, Kovacs EJ, Advanced age impairs macrophage polarization, *Journal of interferon & cytokine research : the official journal of the International Society for Interferon and Cytokine Research*, 32 (2012) 18–26.
- [40]. Bruegmann T, Smith GL, Macrophages: new players in cardiac ageing?, *Cardiovasc Res*, 114 (2018) e47–e49. [PubMed: 29800376]
- [41]. Hachim D, Brown BN, Surface modification of polypropylene for enhanced layer-by-layer deposition of polyelectrolytes, *J Biomed Mater Res A*, 106 (2018) 2078–2085. [PubMed: 29569359]
- [42]. Sacerdote P, Opioids and the immune system, *Palliat Med*, 20 Suppl 1 (2006) s9–15. [PubMed: 16764216]
- [43]. Martucci C, Panerai AE, Sacerdote P, Chronic fentanyl or buprenorphine infusion in the mouse: similar analgesic profile but different effects on immune responses, *Pain*, 110 (2004) 385–392. [PubMed: 15275790]
- [44]. Shukla SK, Mishra AK, Arotiba OA, Mamba BB, Chitosan-based nanomaterials: a state-of-the-art review, *Int J Biol Macromol*, 59 (2013) 46–58. [PubMed: 23608103]
- [45]. Kong M, Chen XG, Xing K, Park HJ, Antimicrobial properties of chitosan and mode of action: a state of the art review, *Int J Food Microbiol*, 144 (2010) 51–63. [PubMed: 20951455]
- [46]. Lee CG, Da Silva CA, Dela Cruz CS, Ahangari F, Ma B, Kang MJ, He CH, Takyar S, Elias JA, Role of chitin and chitinase/chitinase-like proteins in inflammation, tissue remodeling, and injury, *Annu Rev Physiol*, 73 (2011) 479–501. [PubMed: 21054166]
- [47]. den Dekker E, Grefte S, Huijs T, ten Dam GB, Versteeg EM, van den Berk LC, Bladergroen BA, van Kuppevelt TH, Figdor CG, Torensma R, Monocyte cell surface glycosaminoglycans positively modulate IL-4-induced differentiation toward dendritic cells, *J Immunol*, 180 (2008) 3680–3688. [PubMed: 18322173]
- [48]. Trowbridge JM, Gallo RL, Dermatan sulfate: new functions from an old glycosaminoglycan, *Glycobiology*, 12 (2002) 117R–125R.
- [49]. Yu T, Wang W, Nassiri S, Kwan T, Dang C, Liu W, Spiller KL, Temporal and spatial distribution of macrophage phenotype markers in the foreign body response to glutaraldehyde-crosslinked gelatin hydrogels, *J Biomater Sci Polym Ed*, 27 (2016) 721–742. [PubMed: 26902292]
- [50]. Julier Z, Park AJ, Briquez PS, Martino MM, Promoting tissue regeneration by modulating the immune system, *Acta Biomater*, 53 (2017) 13–28. [PubMed: 28119112]
- [51]. Liang R, Abramowitch S, Knight K, Palcsey S, Nolfi A, Feola A, Stein S, Moalli PA, Vaginal degeneration following implantation of synthetic mesh with increased stiffness, *BJOG*, 120 (2013) 233–243. [PubMed: 23240802]
- [52]. Jiang X, Sato T, Yao Z, Keeney M, Pajarinen J, Lin TH, Loi F, Egashira K, Goodman S, Yang F, Local delivery of mutant CCL2 protein-reduced orthopaedic implant wear particle-induced osteolysis and inflammation in vivo, *Journal of orthopaedic research : official publication of the Orthopaedic Research Society*, 34 (2016) 58–64. [PubMed: 26174978]
- [53]. Pajarinen J, Jamsen E, Kontinen YT, Goodman SB, Innate immune reactions in septic and aseptic osteolysis around hip implants, *Journal of long-term effects of medical implants*, 24 (2014) 283–296. [PubMed: 25747031]
- [54]. Sato T, Pajarinen J, Behn A, Jiang X, Lin TH, Loi F, Yao Z, Egashira K, Yang F, Goodman SB, The Effect of Local IL-4 Delivery or CCL2 Blockade on Implant Fixation and Bone Structural Properties in a Mouse Model of Wear Particle Induced Osteolysis, *J Biomed Mater Res A*, (2016).
- [55]. Keeney M, Waters H, Barcay K, Jiang X, Yao Z, Pajarinen J, Egashira K, Goodman SB, Yang F, Mutant MCP-1 protein delivery from layer-by-layer coatings on orthopedic implants to modulate inflammatory response, *Biomaterials*, 34 (2013) 10287–10295. [PubMed: 24075408]

- [56]. Pinchuk LM, Filipov NM, Differential effects of age on circulating and splenic leukocyte populations in C57BL/6 and BALB/c male mice, *Immun Ageing*, 5 (2008) 1. [PubMed: 18267021]
- [57]. Jackson SJ, Andrews N, Ball D, Bellantuono I, Gray J, Hachoumi L, Holmes A, Latcham J, Petrie A, Potter P, Rice A, Ritchie A, Stewart M, Strepka C, Yeoman M, Chapman K, Does age matter? The impact of rodent age on study outcomes, *Lab Anim*, 51 (2017) 160–169. [PubMed: 27307423]
- [58]. Lohmann N, Schirmer L, Atallah P, Wandel E, Ferrer RA, Werner C, Simon JC, Franz S, Freudenberg U, Glycosaminoglycan-based hydrogels capture inflammatory chemokines and rescue defective wound healing in mice, *Sci Transl Med*, 9 (2017).
- [59]. LoPresti ST, Brown BN, Effect of Source Animal Age upon Macrophage Response to Extracellular Matrix Biomaterials, *J Immunol Regen Med*, 1 (2018) 57–66. [PubMed: 30101208]
- [60]. Sanada F, Taniyama Y, Muratsu J, Otsu R, Shimizu H, Rakugi H, Morishita R, Source of Chronic Inflammation in Aging, *Front Cardiovasc Med*, 5 (2018) 12. [PubMed: 29564335]
- [61]. Franceschi C, Campisi J, Chronic inflammation (inflammaging) and its potential contribution to age-associated diseases, *J Gerontol A Biol Sci Med Sci*, 69 Suppl 1 (2014) S4–9. [PubMed: 24833586]
- [62]. Low QE, Drugea IA, Duffner LA, Quinn DG, Cook DN, Rollins BJ, Kovacs EJ, DiPietro LA, Wound healing in MIP-1 α ($-/-$) and MCP-1($-/-$) mice, *Am J Pathol*, 159 (2001) 457–463. [PubMed: 11485904]
- [63]. Boring L, Gosling J, Chensue SW, Kunkel SL, Farese RV Jr., Broxmeyer HE, Charo IF, Impaired monocyte migration and reduced type 1 (Th1) cytokine responses in C-C chemokine receptor 2 knockout mice, *J Clin Invest*, 100 (1997) 2552–2561. [PubMed: 9366570]
- [64]. Kurihara T, Warr G, Loy J, Bravo R, Defects in macrophage recruitment and host defense in mice lacking the CCR2 chemokine receptor, *J Exp Med*, 186 (1997) 1757–1762. [PubMed: 9362535]
- [65]. Kuziel WA, Morgan SJ, Dawson TC, Griffin S, Smithies O, Ley K, Maeda N, Severe reduction in leukocyte adhesion and monocyte extravasation in mice deficient in CC chemokine receptor 2, *Proc Natl Acad Sci U S A*, 94 (1997) 12053–12058. [PubMed: 9342361]
- [66]. Jablonski KA, Amici SA, Webb LM, Ruiz-Rosado Jde D, Popovich PG, Partida-Sanchez S, Guerau-de-Arellano M, Novel Markers to Delineate Murine M1 and M2 Macrophages, *PLoS One*, 10 (2015) e0145342. [PubMed: 26699615]
- [67]. Patel AA, Zhang Y, Fullerton JN, Boelen L, Rongvaux A, Maini AA, Bigley V, Flavell RA, Gilroy DW, Asquith B, Macallan D, Yona S, The fate and lifespan of human monocyte subsets in steady state and systemic inflammation, *J Exp Med*, 214 (2017) 1913–1923. [PubMed: 28606987]
- [68]. Deshmane SL, Kremlev S, Amini S, Sawaya BE, Monocyte chemoattractant protein-1 (MCP-1): an overview, *J Interferon Cytokine Res*, 29 (2009) 313–326. [PubMed: 19441883]
- [69]. Shen JZ, Morgan J, Tesch GH, Fuller PJ, Young MJ, CCL2-dependent macrophage recruitment is critical for mineralocorticoid receptor-mediated cardiac fibrosis, inflammation, and blood pressure responses in male mice, *Endocrinology*, 155 (2014) 1057–1066. [PubMed: 24428529]
- [70]. Gazzaniga S, Bravo AI, Guglielmotti A, van Rooijen N, Maschi F, Vecchi A, Mantovani A, Mordoh J, Wainstok R, Targeting tumor-associated macrophages and inhibition of MCP-1 reduce angiogenesis and tumor growth in a human melanoma xenograft, *J Invest Dermatol*, 127 (2007) 2031–2041. [PubMed: 17460736]
- [71]. Laskin DL, Sunil VR, Gardner CR, Laskin JD, Macrophages and tissue injury: agents of defense or destruction?, *Annu Rev Pharmacol Toxicol*, 51 (2011) 267–288. [PubMed: 20887196]
- [72]. Blau HM, Cosgrove BD, Ho AT, The central role of muscle stem cells in regenerative failure with aging, *Nat Med*, 21 (2015) 854–862. [PubMed: 26248268]
- [73]. Franceschi C, Garagnani P, Parini P, Giuliani C, Santoro A, Inflammaging: a new immune-metabolic viewpoint for age-related diseases, *Nat Rev Endocrinol*, 14 (2018) 576–590. [PubMed: 30046148]
- [74]. Schneemann M, Schoeden G, Macrophage biology and immunology: man is not a mouse, *Journal of leukocyte biology*, 81 (2007) 579; discussion 580.

- [75]. Haley PJ, Species differences in the structure and function of the immune system, *Toxicology*, 188 (2003) 49–71. [PubMed: 12748041]
- [76]. Doeing DC, Borowicz JL, Crockett ET, Gender dimorphism in differential peripheral blood leukocyte counts in mice using cardiac, tail, foot, and saphenous vein puncture methods, *BMC Clin Pathol*, 3 (2003) 3. [PubMed: 12971830]
- [77]. Martinez FO, Gordon S, Locati M, Mantovani A, Transcriptional profiling of the human monocyte-to-macrophage differentiation and polarization: new molecules and patterns of gene expression, *J Immunol*, 177 (2006) 7303–7311. [PubMed: 17082649]
- [78]. Raes G, Brys L, Dahal BK, Brandt J, Grooten J, Brombacher F, Vanham G, Noel W, Bogaert P, Boonefaes T, Kindt A, Van den Bergh R, Leenen PJ, De Baetselier P, Ghassabeh GH, Macrophage galactose-type C-type lectins as novel markers for alternatively activated macrophages elicited by parasitic infections and allergic airway inflammation, *Journal of leukocyte biology*, 77 (2005) 321–327. [PubMed: 15591125]
- [79]. Wang RM, Johnson TD, He J, Rong Z, Wong M, Nigam V, Behfar A, Xu Y, Christman KL, Humanized mouse model for assessing the human immune response to xenogeneic and allogeneic decellularized biomaterials, *Biomaterials*, 129 (2017) 98–110. [PubMed: 28334641]
- [80]. Chung L, Maestas DR Jr., Housseau F, Elisseff JH, Key players in the immune response to biomaterial scaffolds for regenerative medicine, *Adv Drug Deliv Rev*, 114 (2017) 184–192. [PubMed: 28712923]

Highlights

- Layer by layer can provide concomitant and sequential delivery of MCP-1 and IL-4.
- In young mice, single IL-4 delivery shifts the host response to an M2 phenotype.
- In aged mice, single IL-4 delivery does NOT shift the response to an M2 phenotype.
- In aged mice, sequential delivery restores macrophage recruitment.
- In aged mice, sequential delivery shifts the host response to an M2 phenotype.

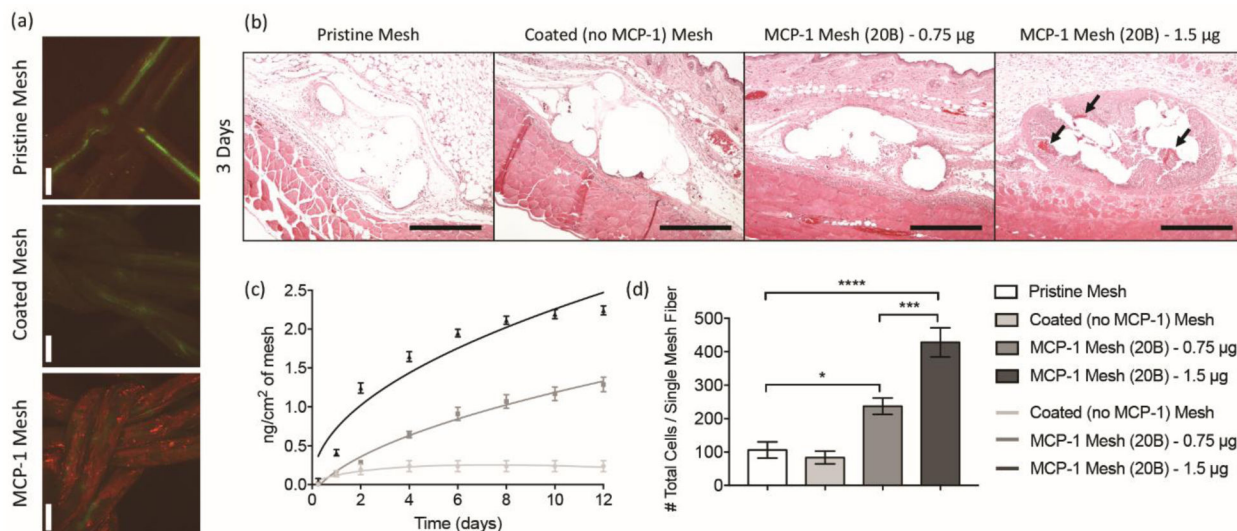


Figure 1.

[a] Confocal microscopy images of MCP-1 immunolabeled (red) polypropylene fibers (green) of pristine (i), coated [no cytokine] (ii) and MCP-1 loaded [20B] (iii) mesh. Scale bars represent 100 µm. [b] H&E stained tissue sections at 10X from mice implanted with a 1 cm² piece of pristine, coated (no cytokine), MCP-1 (0.75 and 1.5 µg/mL in coating solutions, 20B) at 3 days post-implantation. Scale bars represent 200 µm. Arrows indicate mesh erosion. [c] Cumulative release of MCP-1 (nanograms) versus time (days) from 1 cm² pieces of coated mesh loaded with 0.75 and 1.5 µg/mL of MCP-1 (20B). Coated (no cytokine) mesh was used as a control. Points represent the mean ± SEM. [d] Image analysis of total cells (DAPI) surrounding single mesh fibers of tissue cross sections of mice implanted with MCP-1 eluting meshes and controls, 3 days post-implantation. Bars represent the mean ± SEM. Statistical significance as (*) $p < 0.05$, (***) $p < 0.001$ and (****) $p < 0.0001$, using two-way ANOVA with Tukey's tests. All other differences are non-significant.

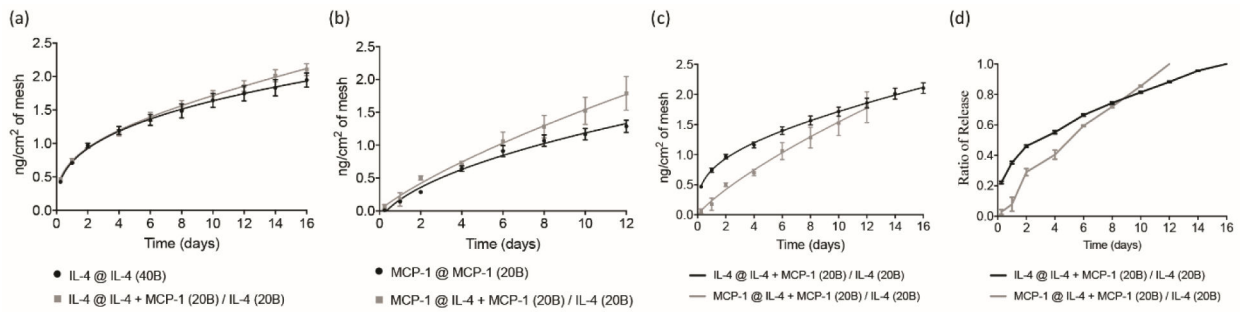


Figure 2.

[a] Cumulative release of IL-4 (nanograms) versus time (days) from eluting meshes containing 40 bilayers of IL-4 (black curve) and 20 bilayers of MCP-1/IL-4 plus 20 bilayers of IL-4 (gray curve). [b] Cumulative release of MCP-1 (nanograms) versus time (days) from eluting meshes containing 20 bilayers of MCP-1 (black curve) and 20 bilayers of MCP-1/IL-4 plus 20 bilayers of IL-4 (gray curve). [c] Cumulative release of MCP-1 (gray curve) and IL-4 (black curve) versus time (days) from eluting meshes containing 20 bilayers of MCP-1/IL-4 plus 20 bilayers of IL-4. [d] Ratio of released MCP-1 and IL-4 (nanograms) versus time (days) from eluting meshes containing 20 bilayers of MCP-1/IL-4 plus 20 bilayers of IL-4. Points represent the mean \pm SEM.

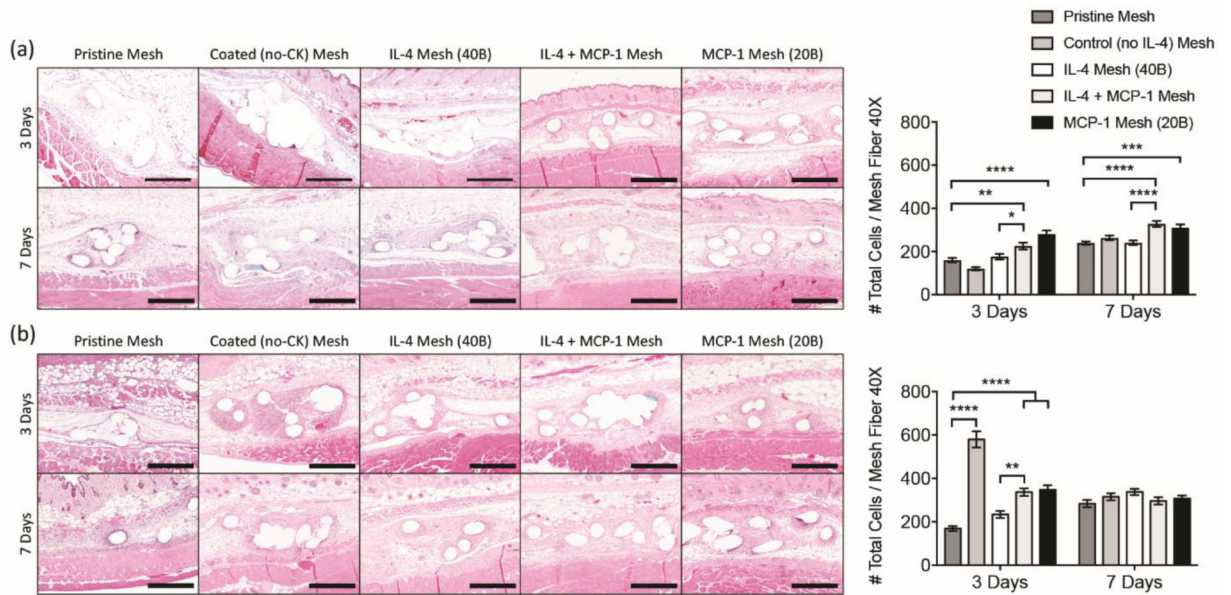


Figure 3.

Images of H&E stained tissue cross sections (10X) and total cell counts (DAPI) surrounding single mesh fibers (40X) at 3 and 7 days from [a] young and [b] aged mice implanted with a 1 cm² piece of pristine, coated (no cytokine), single and sequential MCP-1 and IL-4 eluting meshes. Scale bars represent 200 μ m. Bars represent the mean \pm SEM. Statistical significance as (*) $p < 0.05$, (**) $p < 0.01$, (***) $p < 0.001$ and (****) $p < 0.0001$, using two-way ANOVA with Tukey's tests. All other differences are non-significant.

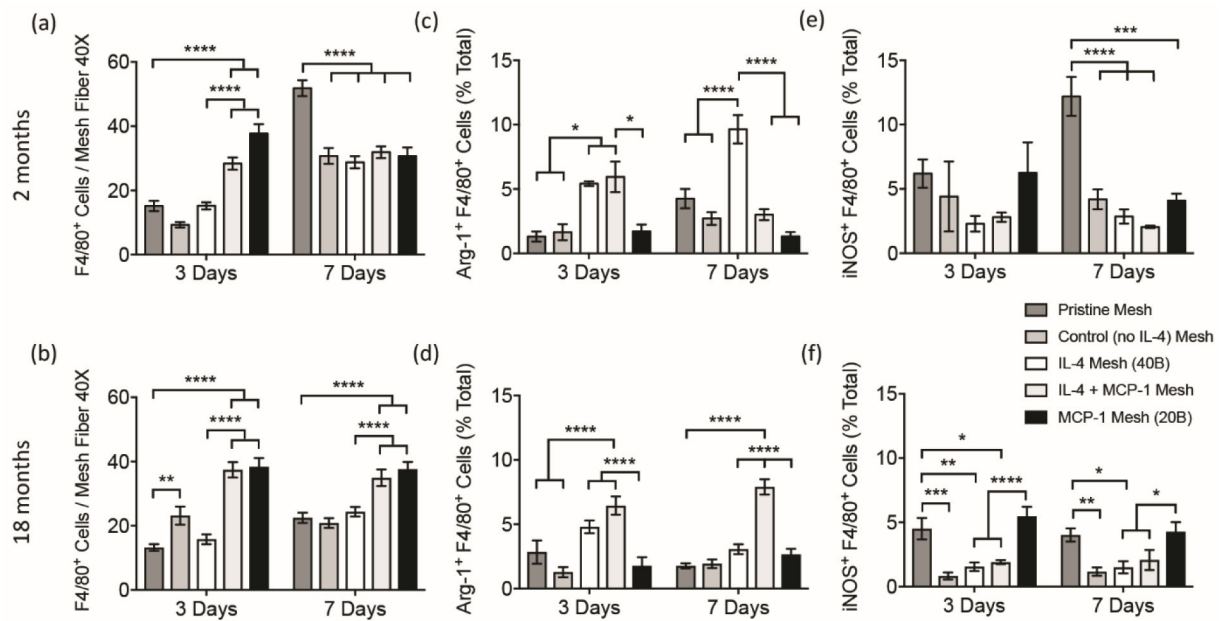


Figure 4.

Image analysis of total F4/80⁺ macrophages [a, b], Arg-1⁺ F4/80⁺ (M2) macrophages [c, d] and iNOS⁺ F4/80⁺ (M1) macrophages [e, f] surrounding single mesh fibers of co-immunolabelled tissue cross sections from young [a, c, e] and aged [b, d, f] mice implanted with a 1 cm² piece of pristine, coated (no cytokine), single and sequential MCP-1 and IL-4 eluting meshes, 3 and 7 days post-implantation. Bars represent the mean \pm SEM (N = 5). Statistical significance as (*) p < 0.05, (**) p < 0.01, (***) p < 0.001 and (****) p < 0.0001, using two-way ANOVA with Tukey's (groups) and Sidak's (days) tests. All other differences are non-significant.

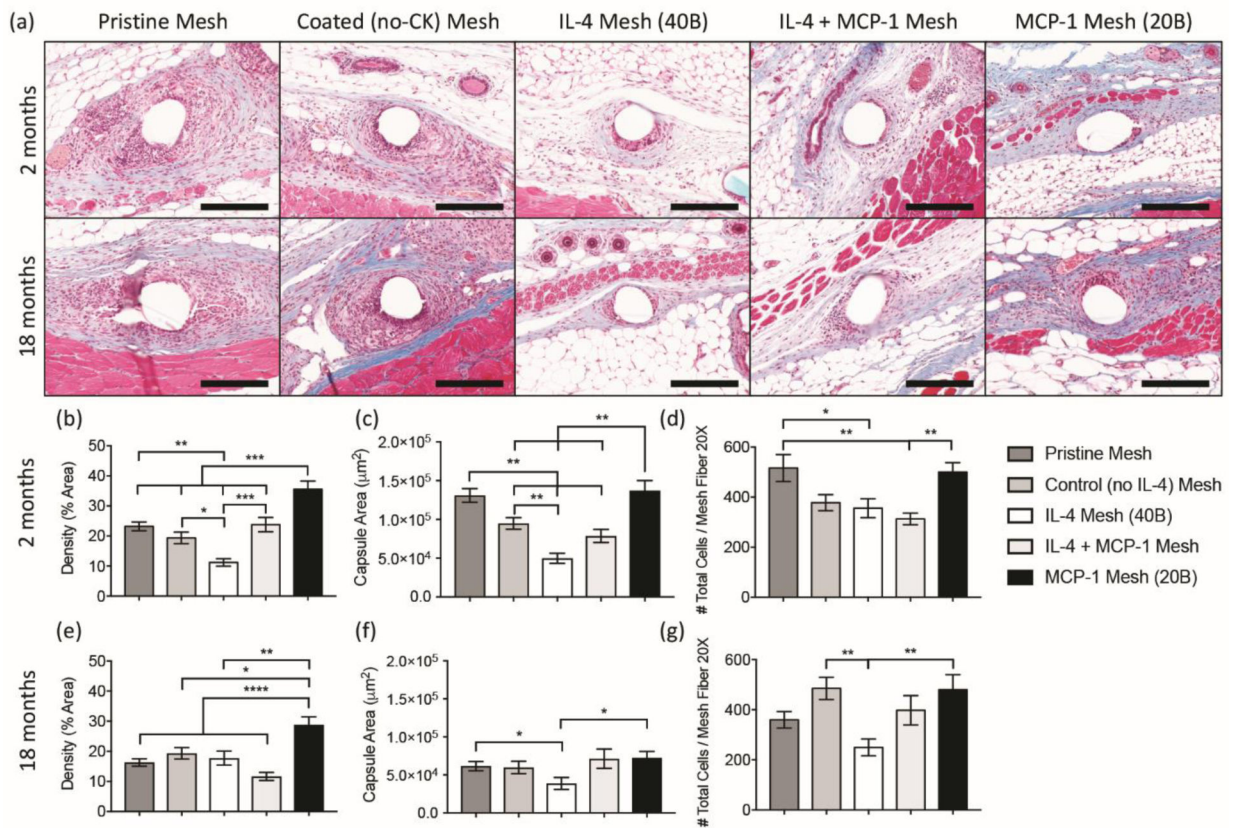


Figure 5.

[a] Masson's Trichrome stained tissue sections of young and aged mice implanted with a 1 cm^2 piece of pristine, coated (no cytokine), single and sequential MCP-1 and IL-4 eluting meshes, 90 days post-implantation. [b] Image analysis of capsule density [area %; b, e], capsule area [μm^2 ; c, f] and total cell number [d, g] on single mesh fibers (20X) from young [b – d] and aged [e – g] mice. Bars represent the mean \pm SEM. Statistical significance as (*) $p < 0.05$, (**) $p < 0.01$, (***) $p < 0.001$ and (****) $p < 0.0001$, using two-way ANOVA with Tukey's test. All other differences are non-significant.